



HAL
open science

Divergent roles of IREG/Ferroportin transporters from the nickel hyperaccumulator *Leucocroton havanensis*

Dubiel Alfonso Gonzalez, Vanesa Sanchez Garcia de la Torre, Rolando Reyes Fernandez, Louise Barreau, Sylvain Merlot

► To cite this version:

Dubiel Alfonso Gonzalez, Vanesa Sanchez Garcia de la Torre, Rolando Reyes Fernandez, Louise Barreau, Sylvain Merlot. Divergent roles of IREG/Ferroportin transporters from the nickel hyperaccumulator *Leucocroton havanensis*. *Physiologia Plantarum*, 2024, 176, pp.e14261. 10.1111/ppl.14261 . hal-04274029v2

HAL Id: hal-04274029

<https://hal.science/hal-04274029v2>

Submitted on 20 Sep 2024

HAL is a multi-disciplinary open access archive for the deposit and dissemination of scientific research documents, whether they are published or not. The documents may come from teaching and research institutions in France or abroad, or from public or private research centers.




L'archive ouverte pluridisciplinaire **HAL**, est destinée au dépôt et à la diffusion de documents scientifiques de niveau recherche, publiés ou non, émanant des établissements d'enseignement et de recherche français ou étrangers, des laboratoires publics ou privés.



Distributed under a Creative Commons Attribution - NonCommercial - NoDerivatives 4.0 International License

ORIGINAL RESEARCH

Divergent roles of IREG/Ferroportin transporters from the nickel hyperaccumulator *Leucocroton havanensis*

Dubiel Alfonso González^{1,2}  | Vanesa Sánchez García de la Torre³  |
 Rolando Reyes Fernández²  | Louise Barreau³ | Sylvain Merlot^{3,4} 

¹Jardín Botánico Nacional, Universidad de La Habana, La Habana, Cuba

²Universidad Agraria de La Habana, Facultad de Agronomía, San José de las Lajas, Mayabeque, Cuba

³Université Paris-Saclay, CEA, CNRS, Institute for Integrative Biology of the Cell (I2BC), Gif-sur-Yvette, France

⁴Laboratoire de Recherche en Sciences Végétales (LRSV), UMR5546 CNRS/UPS/INPT, France

Correspondence

Dubiel Alfonso González,
 Email: dubiel.alfonso@gmail.com

Sylvain Merlot,
 Email: sylvain.merlot@univ-tlse3.fr

Funding information

French Embassy in Cuba - SCAC mobility fellowship; Centre National de la Recherche Scientifique, Grant/Award Number: MITI Defi Enviromics GENE-4-CHEM; Agence Nationale de la Recherche, Grant/Award Number: ANR-13-ADAP-0004

Edited by K.-J. Dietz

Abstract

In response to our ever-increasing demand for metals, phytotechnologies are being developed to limit the environmental impact of conventional metal mining. However, the development of these technologies, which rely on plant species able to tolerate and accumulate metals, is partly limited by our lack of knowledge of the underlying molecular mechanisms. In this work, we aimed to better understand the role of metal transporters of the IRON REGULATED 1/FERROPORTIN (IREG/FPN) family from the nickel hyperaccumulator *Leucocroton havanensis* from the Euphorbiaceae family. Using transcriptomic data, we identified two homologous genes, *LhavIREG1* and *LhavIREG2*, encoding divalent metal transporters of the IREG/FPN family. Both genes are expressed at similar levels in shoots, but *LhavIREG1* shows higher expression in roots. The heterologous expression of these transporters in *A. thaliana* revealed that *LhavIREG1* is localized to the plasma membrane, whereas *LhavIREG2* is located on the vacuole. In addition, the expression of each gene induced a significant increase in nickel tolerance. Taken together, our data suggest that *LhavIREG2* is involved in nickel sequestration in vacuoles of leaf cells, whereas *LhavIREG1* is mainly involved in nickel translocation from roots to shoots, but could also be involved in metal sequestration in cell walls. Our results suggest that paralogous IREG/FPN transporters may play complementary roles in nickel hyperaccumulation in plants.

1 | INTRODUCTION

Since the beginning of the industrial revolution, and today, accelerated by the energy transition required to reduce CO₂ emissions, the use of metals has increased exponentially for strategic metals. Metal mining and refining are responsible for the dispersion of metals from primary sites, increasing the risk of contamination in the natural environment and agricultural soils (Dudka and Adriano 1997; Li et al. 2014; Sonter et al. 2020; Vidal et al. 2022). Phytotechnologies based on plants capable of hyperaccumulating metals have been proposed as a solution to limit the environmental impact of metal mining,

remediate contaminated soils and recycle valuable metals (Suman et al. 2018; DalCorso et al. 2019; Corzo Remigio et al. 2020). The development of these phytotechnologies is particularly relevant in Mediterranean and tropical regions where nickel mining can have a significant impact on rich biodiversity (van der Ent et al. 2015). As for other crops, a better understanding of the molecular mechanisms involved in metal tolerance and accumulation will support the development of sustainable phytotechnologies using hyperaccumulators.

Metal hyperaccumulators are plant species that are able to tolerate and accumulate enormous amounts of metal in their leaves (van der Ent et al. 2013). More than 700 hyperaccumulators have been

This is an open access article under the terms of the [Creative Commons Attribution-NonCommercial-NoDerivs](https://creativecommons.org/licenses/by-nc-nd/4.0/) License, which permits use and distribution in any medium, provided the original work is properly cited, the use is non-commercial and no modifications or adaptations are made.

© 2024 The Authors. *Physiologia Plantarum* published by John Wiley & Sons Ltd on behalf of Scandinavian Plant Physiology Society.

identified, accumulating a wide variety of metals such as nickel, zinc or manganese. However, nickel hyperaccumulators represent the vast majority of these species (Reeves et al. 2018). At the molecular level, metal hyperaccumulation requires high activity of genes involved in metal chelation and transport, from metal uptake by roots to metal storage in leaves (Manara et al. 2020). Accordingly, molecular studies, mostly performed in hyperaccumulators from the Brassicaceae family, suggest that metal hyperaccumulation has evolved from the high and constitutive expression of genes involved in the regulation of metal homeostasis in plants (Becher et al. 2004; Weber et al. 2004; Hammond et al. 2006; Halimaa et al. 2014). For example, zinc hyperaccumulation in *Arabidopsis halleri* has evolved from the triplication of the *HEAVY METAL ATPase 4* (*AhHMA4*) gene and mutations in *cis*-elements leading to high expression of this metal pump. The high activity of *AhHMA4* promotes zinc loading in the xylem and, thus, efficient translocation of zinc to the shoots (Hanikenne et al. 2008). Interestingly, similar genetic mechanisms are proposed to be at the origin of zinc hyperaccumulation in *Noccaea caerulescens*, suggesting that the high expression of *HMA4* is a convergent mechanism involved in zinc hyperaccumulation in Brassicaceae (Ó Lochlainn et al. 2011; Craciun et al. 2012). Recent studies have shown that the high expression of divalent metal ion transporters of the IRON REGULATED 1/FERROPORTIN family (IREG/FPN) is repeatedly associated with nickel hyperaccumulation in several plant families (Halimaa et al. 2014; Merlot et al. 2014; Meier et al. 2018; García de la Torre et al. 2021).

In plant genomes, IREG/FPN transporters fall into two clades (Schaaf et al. 2006; García de la Torre et al. 2021). The first clade, hereafter called group 1 and represented by *Arabidopsis thaliana* AtIREG3/MAR1, encodes plastid-targeted transporters that are likely involved in the regulation of iron homeostasis in chloroplasts and mitochondria (Conte et al. 2009; Kim et al. 2021). The second group, hereafter named group 2 and represented by AtIREG1/FPN1 and AtIREG2/FPN2 in *A. thaliana*, encodes vacuolar and plasma membrane transporters (Schaaf et al. 2006; Morrissey et al. 2009). AtIREG2/FPN2 was shown to be expressed in roots in response to iron starvation and localized to the vacuolar membrane. The *A. thaliana ireg2* mutant is more sensitive to nickel, suggesting that AtIREG2 transports nickel into vacuoles to limit metal toxicity. Accordingly, plants overexpressing AtIREG2 are more resistant to nickel and accumulate more of this metal (Schaaf et al. 2006). In contrast, AtIREG1/FPN1 localizes to the plasma membrane and has been proposed to mediate cobalt loading into the xylem for long-distance transport to the shoot (Morrissey et al. 2009). However, the *ireg1* mutation further increases the nickel sensitivity associated with *ireg2*, suggesting that AtIREG1 is also capable of transporting nickel. Analysis of orthologous transporters from *Medicago truncatula* (MtFPN2) and from *rice* (OsFPN1) revealed that IREG/FPN transporters belonging to group 2 can also localize in endomembranes and Golgi respectively (Escudero et al. 2020; Kan et al. 2022).

To date, the functional analyses of IREG/FPN transporters associated with nickel hyperaccumulation have suggested that these transporters are involved in the storage of nickel in the vacuole of leaf cells (Merlot et al. 2014; García de la Torre et al. 2021). However, the

genome of several nickel hyperaccumulators contains more than one gene encoding for group 2 IREG/FPN transporters. Interestingly, the nickel hyperaccumulator *Leucocroton havanensis*, endemic to Cuba, expresses two genes coding for group 2 IREG/FPN transporters in leaves, *LhavIREG1* and *LhavIREG2*, whereas the related non-accumulator species *Leucocroton microphyllus* apparently expresses only one gene, *LmicIREG1*, to a lower level (García de la Torre et al. 2021). This observation raises the question of the respective role of distinct group 2 IREG/FPN transporters in nickel hyperaccumulation.

In this work, we have studied the function of the *LhavIREG1* and *LhavIREG2* transporters from the nickel hyperaccumulator *L. havanensis*. Our results indicate that the two genes have distinct expression patterns in roots and shoots of *L. havanensis* and localize to different cellular membranes. Heterologous expression in *A. thaliana* further suggests that the two genes have different functions in nickel transport and may therefore play distinct but complementary roles in nickel tolerance and accumulation.

2 | MATERIALS AND METHODS

2.1 | Plant material

Leucocroton havanensis seeds were collected from a single female specimen (23°04'55.5"N 82°06'46.1"W) growing on ultramafic soil in the ecological reserve "La Coca" (Havana, Cuba). Seeds and young plantlets were grown *in vitro* on Murashige and Skoog agar medium supplemented or not with 3.2 mM NiSO₄ for 6 weeks after germination as previously described (González and Matrella 2013). Root and shoot samples were collected separately and washed with distilled water. After rapidly removing water with a paper towel, samples were cut into 3 mm pieces and immediately placed in RNAlater (Sigma-Aldrich). Samples were transported from Cuba to France and stored at −80°C until processing.

2.2 | Transcriptomic analyses

RNA from *L. havanensis* root and shoot samples treated or not with nickel were extracted using Tri reagent (Sigma-Aldrich). RNA sequencing, *de novo* transcriptome assembly, transcriptome annotation, read mapping and differential gene expression analysis were performed essentially as described previously (García de la Torre et al. 2021). The *de novo* assembly of the transcriptome (*Lhav_v2*) was performed using RNA-seq reads from root and shoot samples of nickel-treated plantlets. The quality of the assembly was analyzed by the TransRate v1.0.3 package using the trimmed read sequences used to assemble *Lhav_v2* (Smith-Unna et al. 2016). The completeness of the assembled transcriptome was estimated using BUSCO (v 4.0.6) and viridiplantae_odb10 lineage dataset (Seppey et al. 2019). Differential gene expression analysis was performed using the edgeR bioconductor package with TMM normalization and Exact test for statistical analysis, with one repetition per sample. Genes with absolute fold change

|FC| ≥ 10 and adjusted p-value ≤ 0.05 were considered as differentially expressed (DE) genes. Enrichment analysis was performed using Mercator4 v.4 (Schwacke et al. 2019).

2.3 | Reconstruction and cloning of *LhaviREG* coding sequences

The coding sequence of *LhaviREG1* was predicted from transcriptome Lhav_v2 contigs #981 and #4486, and from transcriptome Lhav_v1 contigs #820 and #4646. The coding sequence of *LhaviREG2* was predicted from transcriptome Lhav_v2 contig #101 and from transcriptome Lhav_v1 contigs #170 and #14018. The coding sequence of *LhaviREG3* was predicted from transcriptome Lhav_v2 contigs #6824 and #12273, and from transcriptome Lhav_v1 contigs #8277, #9347 and #4646.

The coding sequences of *LhaviREG1* and *LhaviREG2* were amplified from leaf cDNA using high-fidelity Phusion polymerase (Thermo Scientific) with gene-specific primers containing the attB recombination sequences attB1_*LhaviREG1*_For/attB2_*LhaviREG1*_Rev-(no) stop and attB1_*LhaviREG2*_For/attB2_*LhaviREG2*_Rev-(no)stop, respectively (Table S1). The PCR products were recombined into pDONR207 using GATEWAY technology (Invitrogen) to generate pDON207-*LhaviREG1*(no)stop and pDON207-*LhaviREG2*(no)stop. We confirmed the predicted sequences of the *LhaviREG1* and *LhaviREG2* coding regions by double-strand Sanger sequencing (GATC-Eurofins).

2.4 | Phylogenetic analysis

Sequences for IREG/FPN proteins were obtained from Dicots Plaza 5.0 (Van Bel et al. 2022), for *Arabidopsis thaliana* AthalREG1 (AT2G38460), AthalREG2 (AT5G03570), AthalREG3 (AT5G26820); *Arabidopsis lyrata* AlyriREG1 (AL4G35730), AlyriREG2 (AL6G13070), AlyriREG3 (AL6G38700); *Eutrema salsugineum* EsallREG1 (Thhalv10013299m.g), EsallREG2 (Thhalv10016525m.g), EsallREG3 (Thhalv10003867m.g); *Teobroma cacao* TcaclREG1 (Thecc.05G005200), TcaclREG2 (Thecc.05G005300), TcaclREG3 (Thecc.05G323900); *Cucumis melo* CmelREG1 (MELO3C026034.2), CmelREG3 (MELO3C004177.2); *Phaseolus vulgaris* PvullREG1 (Phvul.010G062200), PvullREG2 (Phvul.010G062300), PvullREG3 (Phvul.007G201800); *Nicotiana tabacum* NtablREG1 (Nitab4.5_0000355g0170), NtablREG2 (Nitab4.5_0012987g0010), NtablREG3_1 (Nitab4.5_0001338g0110), NtablREG3_2 (Nitab4.5_0004525g0030); *Chenopodium quinoa* CquillREG1 (AUR62006302), CquillREG2 (AUR62026347), CquillREG3_1 (AUR62000385), CquillREG3_2 (AUR62006741) and *Erigeron canadensis* EcanIREG1 (ECA247G0592). The sequences of *Ricinus communis* RcomIREG1 (XP_048225718.1), RcomIREG2 (XP_048235846.1), RcomIREG3 (XP_002512519.1) and *Homo sapiens* HsapFPN (XP_047300022.1) were obtained from NCBI. The sequences of *Leucocroton havanensis* LhavIREG1 and LhavIREG2 proteins were translated from the corresponding cDNA sequences (OR234317,

OR234318). The sequence of LhavIREG3 was deduced from the corresponding contigs. Protein alignment was performed with CLC Genomics Workbench 22.0.1 (Qiagen) using MUSCLE v3.8.425 (Edgar 2004). The tree was constructed using maximum likelihood phylogeny (neighbor-joining, 100 bootstrap replicates) and displayed using iTol v6 (Letunic and Bork 2021).

2.5 | Quantification of gene expression by RT-qPCR

Total RNA was extracted with TRI reagent according to the manufacturer's instructions (Sigma-Aldrich) and purified with RNeasy Plant Mini Kit on-column DNase I treatment (Qiagen). cDNA synthesis, quantitative PCR amplification and analysis were performed as previously described (García de la Torre et al. 2021). The expression of *LhaviREG1* and *LhaviREG2* was normalized to the expression of the *HISTIDINE KINASE 3* gene (*LhavH3K*; Lhav_v2 contig #1232), which was chosen as a reference because of its stable expression in our transcriptomic data. Primers used for RT-qPCR experiments are given in Table S1. The relative expression of *LhaviREG1* and *LhaviREG2* was quantified according to Pfaffl (2001).

2.6 | Analysis of *LhaviREG1* and *LhaviREG2* activity in yeast

pDON207-*LhaviREG1*stop and pDON207-*LhaviREG2*stop were recombined with pDR195-GTW (Oomen et al. 2009) to generate pDR195-*LhaviREG1* and pDR195-*LhaviREG2*. These constructs were transformed together with pDR195-GTW and pDR195-*AtIREG2* (Schaaf et al. 2006) into *Saccharomyces cerevisiae* strain Y00000H strain (BY4741; MATa; *leu2Δ*; *met15Δ*; *ura3Δ*). Nickel accumulation in yeast was essentially determined as previously described (Merlot et al. 2014; García de la Torre et al. 2021). Yeast cells were grown in 50 mL of liquid SD-Ura medium supplemented with 400 μ M NiCl₂ for 30 h at 28°C with vigorous shaking. Cells were harvested by centrifugation at 4°C and pellets were washed twice with ice-cold [10 mM EDTA, 20 mM MES pH 5.5] and once with ice-cold ultrapure water. Pellets were dried at 65°C prior to elemental analysis (see after).

2.7 | Expression of *LhaviREG1* and *LhaviREG2* in *Arabidopsis thaliana*

pDON207-*LhaviREG1*nostop and pDON207-*LhaviREG2*nostop were recombined with the plant expression vector pMUBI83 (Merlot et al. 2014) to express C-terminal protein fusions with the green fluorescent protein (GFP) under the control of the *AtUBI10* promoter. Both constructs, *AtUBI10::LhaviREG1*-GFP and *AtUBI10::LhaviREG2*-GFP, were transformed into the *A. thaliana ireg2-1* mutant (Schaaf et al. 2006) as described previously (Merlot et al. 2014). For each construct, three homozygous, single locus insertion, T3 lines, expressing

the fluorescent protein were selected. T3 lines together with *ireg2-1* and WT (Col) were grown *in vitro* for 10 days on Hoagland agar medium containing 10 μM Fe-HBED and supplemented with 30 or 50 μM NiCl_2 . Primary root length was measured as described previously (Merlot et al. 2014). To measure metal accumulation, plants were grown on Hoagland agar medium containing 10 μM Fe-HBED for 7 days and then transferred to the same medium supplemented with 50 μM NiCl_2 for 5 days. Roots and shoots samples were washed as previously described (Merlot et al. 2014) before elemental analyses (see after).

2.8 | Quantitative elemental analyses

The dry weight of yeast and plant samples was measured before mineralization in 2 mL of 70% HNO_3 for 4 h at 120°C. Samples were diluted with ultrapure water to a total volume of 12 mL, and metal content was measured using a 4200 MP-AES spectrophotometer (Agilent technologies) as previously described (García de la Torre et al. 2021).

2.9 | Confocal imaging

Roots of *ireg2-1* transgenic T₂ lines expressing *LhaviREG1-GFP* and *LhIREG2-GFP* were imaged on a Leica SP8X inverted confocal microscope (IMAGERIE-Gif platform www.i2bc.paris-saclay.fr/bioimaging/) as previously described (Merlot et al. 2014), with laser excitation at 490 nm and collection of emitted light at 500–550 nm for GFP and 600–650 nm for propidium iodide.

2.10 | Statistics

Statistical analyses were performed using Prism GraphPad (v10.1).

TABLE 1 Parameters of *Leucocroton havanensis* transcriptome assembly (Lhav_v2).

Contig metrics	
Number of contigs	65936
Number over 1 kb	14320
Mean length (kb)	757
N50 (kb)	1196
Read mapping metrics	
Fragment mapped (%)	87
Good mapping (%)	76
Transrate score	
Good contigs (%)	95
Busco score (%)	
	69.6
S: 68.7%, D: 0.9%, F: 25.2%, M: 6.1%	

3 | RESULTS

3.1 | Analysis of shoot and root transcriptomes of *Leucocroton havanensis*

In a previous study, we generated the leaf transcriptome of *Leucocroton havanensis* (Lhav_v1) and compared it with the leaf transcriptome of the related non-accumulator species *Lasiocroton microphyllus* to identify genes associated with the nickel hyperaccumulation trait (García de la Torre et al. 2021). In this study, we wanted to deepen our knowledge of the root and shoot mechanisms involved in nickel hyperaccumulation in *L. havanensis*. We sequenced RNA from roots and shoots to generate a new transcriptome assembly for this nickel hyperaccumulator species (Lhav_v2). This assembly consists of 65 936 contigs with 14 320 contigs larger than 1 kb (Table 1). 31 936 contigs (48%) were annotated with Blast2GO and 12 771 contigs (19%) with Mercator 4. We then used this transcriptome as a reference to analyze the effect of nickel on gene expression in *L. havanensis* (Figure S1, Table S2). We identified 27 contigs differentially expressed (DE; $|\text{FC}| \geq 10$, adj. p-value ≤ 0.05) in response to nickel in roots (Figure S1B), indicating a limited effect of nickel hyperaccumulation on gene expression in this tissue. Enrichment analysis (Table S2) indicated that contigs encoding for seed storage proteins (MapMan4 category 19.5.1) are overrepresented (4 contigs, FDR adj. p-value = 3.1×10^{-7}) among the 19 contigs up-regulated in response to nickel in roots. In contrast, we identified 442 DE contigs in shoots, with 170 contigs up- and 272 contigs down-regulated in response to nickel (Figure S1A). This result suggests that nickel accumulation has a more pronounced effect on the shoot transcriptome. However, we could not identify enriched functional categories among DE contigs in shoots. In particular, we did not identify any DE contigs encoding proteins involved in metal transport or homeostasis.

3.2 | IREG/ferroportin genes expressed in *Leucocroton havanensis*

IREG/FPN transporters have previously been implicated in nickel tolerance and accumulation in plants (Schaaf et al. 2006; Merlot et al. 2014; Meier et al. 2018; García de la Torre et al. 2021). Using *Leucocroton havanensis* transcriptome assemblies, we reconstructed the sequence of IREG/FPN genes expressed in this species. We identified 2 distinct transcripts coding for IREG/FPN transporters orthologous to *A. thaliana* AtIREG1 and AtIREG2. These transporters, named LhavIREG1 and LhavIREG2, belong to the Plaza orthologous group (OG) ORTHO05D005013, which corresponds to group 2 IREG/FPN (Figure 1). We identified a third transporter, LhavIREG3, orthologous to AtIREG3 (belonging to group 1) corresponding to OG ORTHO05D008050. The analysis of the phylogenetic tree obtained with plant IREG/FPN indicates that *LhavIREG1* and *LhavIREG2* originated from a duplication of an IREG/FPN ancestral gene in the Euphorbiaceae family that is independent of the duplication that occurred in the Brassicaceae and gave rise to the paralogous groups represented by AtIREG1 and AtIREG2. It is therefore not possible to

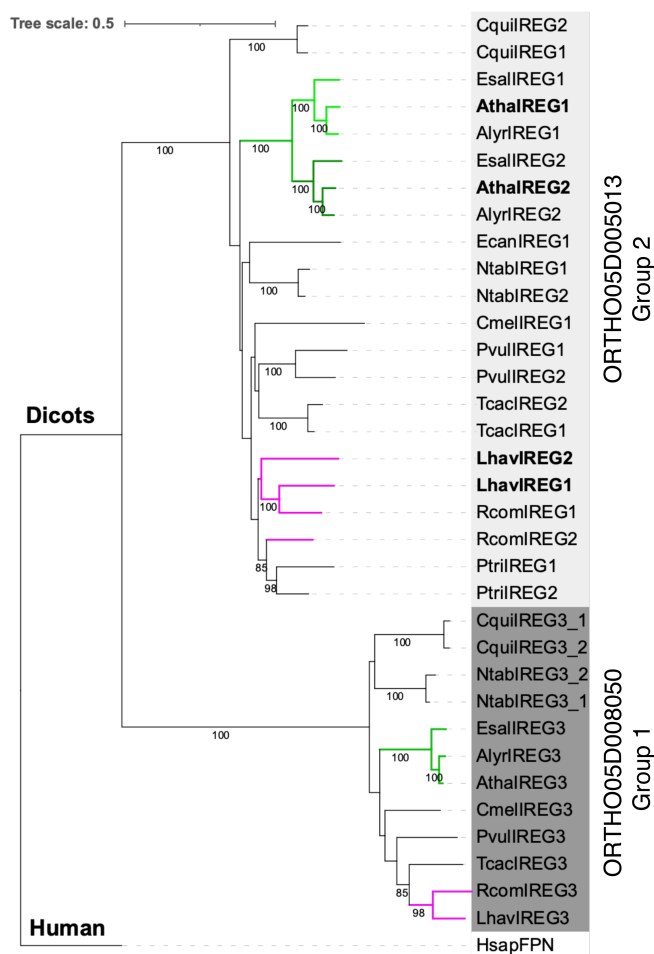


FIGURE 1 Phylogenetic tree of the IREG/FPN metal transporter family from Eudicots. This tree includes IREG/FPN proteins from *Arabidopsis thaliana* (Atha, Brassicaceae), *A. lyrata* (Alyr, Brassicaceae), *Eutrema salsugineum* (Esal, Brassicaceae), *Teobroma cacao* (Tcac, Malvaceae), *Cucumis melo* (Cmel, Cucurbitaceae), *Phaseolus vulgaris* (Pvul, Fabaceae), *Nicotiana tabacum* (Ntab, Solanaceae), *Chenopodium quinoa* (Cqui, Amaranthaceae), *Erigeron canadensis* (Ecan, Asteraceae), *Ricinus communis* (Rcom, Euphorbiaceae), *Leucocroton havanensis* (Lhav, Euphorbiaceae). *Homo sapiens* (Hsap) ferroportin was used as an outgroup. Orthogroups ORTHO05D005013 and ORTHO05D008050 from Plaza 5 are shaded in light and dark gray, respectively. Clades containing Brassicaceae (green) and Euphorbiaceae (magenta) species are highlighted.

infer the function of the *L. havanensis* IREG/FPN transporters from the known function of AtIREG1 and AtIREG2, which act at the plasma membrane and the vacuole respectively (Schaaf et al. 2006; Morrissey et al. 2009).

3.3 | Analysis of LhavIREG1 and LhavIREG2 expression in *Leucocroton havanensis*

Analysis of the RNA-Seq data indicated that both *LhavIREG1* and *LhavIREG2* are expressed at similar levels in shoots but that *LhavIREG1* is more highly expressed than *LhavIREG2* in roots (Figure 2A). These primary observations were largely confirmed by RT-qPCR analyses using

3 independent RNA samples (Figure 2B). These analyses further indicated that nickel treatment resulted in a 3-fold reduction in the expression of both *LhavIREG1* and *LhavIREG2* in shoots. These results suggest that *LhavIREG1* is the major IREG/FPN transporter gene acting in roots of *L. havanensis*, while both genes are likely to have a function in leaves. In this tissue, nickel accumulation may be responsible for a limited down-regulation of the expression of these transporters.

3.4 | LhavIREG1 and LhavIREG2 act as nickel exporters

IREG/FPN are metal exporters that are able to transport several divalent metals (Pan et al. 2020). We have previously shown that the expression of *LhavIREG2* in yeast under the control of the strong *PMA1* promoter increases nickel tolerance (García de la Torre et al. 2021). Here, we observed that the expression of *LhavIREG1* in the same condition does not visibly increase the yeast tolerance to nickel (Figure 3A). To further characterize the activity of *LhavIREG2* and *LhavIREG1*, we measured nickel accumulation in yeast cells expressing each of these transporters (Figure 3B). The expression of *LhavIREG1* or *LhavIREG2* significantly reduces nickel accumulation compared to yeast transformed with the control vector. The same result is observed with *A. thaliana* IREG2. In contrast, we did not measure a significant change in iron accumulation in yeast cells expressing these IREG/FPN genes. These results indicate that the strong expression of *LhavIREG1* or *LhavIREG2* triggers a net transport of nickel out of yeast cells, which is consistent with the conserved role of IREG/FPN as divalent metal exporters. However, differences in the targeting of *LhavIREG1* and *LhavIREG2* in this heterologous expression may affect nickel distribution in yeast cells and, therefore, nickel tolerance.

3.5 | LhavIREG1 and LhavIREG2 localize to different membranes in plant cells

To analyze the localization of *LhavIREG1* and *LhavIREG2* in plant cells, we fused the two transporters with the green fluorescent protein (GFP) at the C-terminal end and expressed the fusion proteins under the control of the *UBI10* promoter in the *A. thaliana* *ireg2* mutant. Root cells of the transgenic T2 lines were imaged by confocal microscopy (Figure 4). Transgenic lines expressing *LhavIREG1*-GFP show a thin GFP fluorescent signal that delineates the periphery of the root cells (Figure 4A, C). In some images, two thin membranes delineating adjacent cells and separated by the cell wall are clearly visible (Figure 4C, D). This localization indicates that *LhavIREG1* is mainly localized to the plasma membrane, although intracellular vesicles can also be labeled with *LhavIREG1*, suggesting cellular trafficking of the transporter (Figure 4C). The fluorescence signal associated with *LhavIREG2*-GFP was weaker than that observed for *LhavIREG1*-GFP. In contrast to *LhavIREG1*-GFP, *LhavIREG2*-GFP outlined large cytoplasmic vesicles that detached from the cell periphery (Figure 4E, F), as previously observed for NcIREG2 in *N. caerulea* and PgIREG1 from *P. gabriellae* (Merlot et al. 2014; García de la Torre et al. 2021).

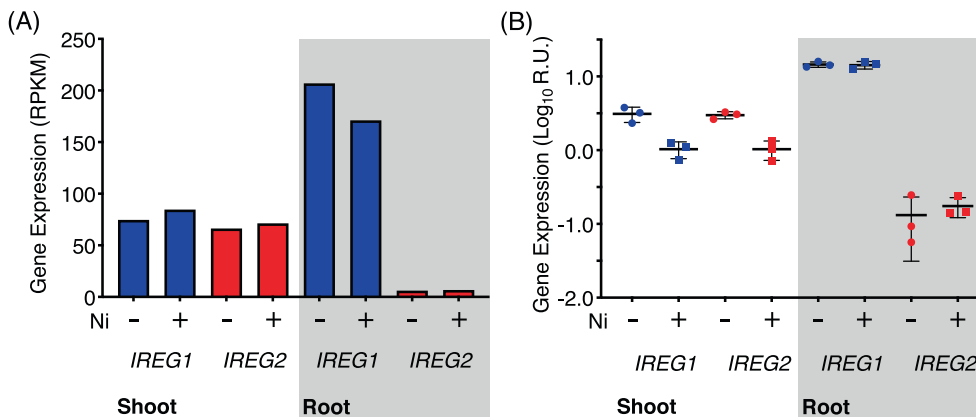


FIGURE 2 Analysis of the expression of *LhaviREG1* and *LhaviREG2* in *Leucocroton havanensis*. (A) The expression of *LhaviREG1* (contig_981) and *LhaviREG2* (contig_101) in response to nickel (Ni) in roots and shoots was extracted from the RNA-Seq experiment and expressed as RPKM after normalization of the expression values. (B) The expression of *LhaviREG1* and *LhaviREG2* was measured by RT-qPCR relative to the expression of the *H3K* gene used as reference. Data are mean value \pm SD ($n = 3$ independent RNA samples per condition) and are presented on a Log₁₀ scale.

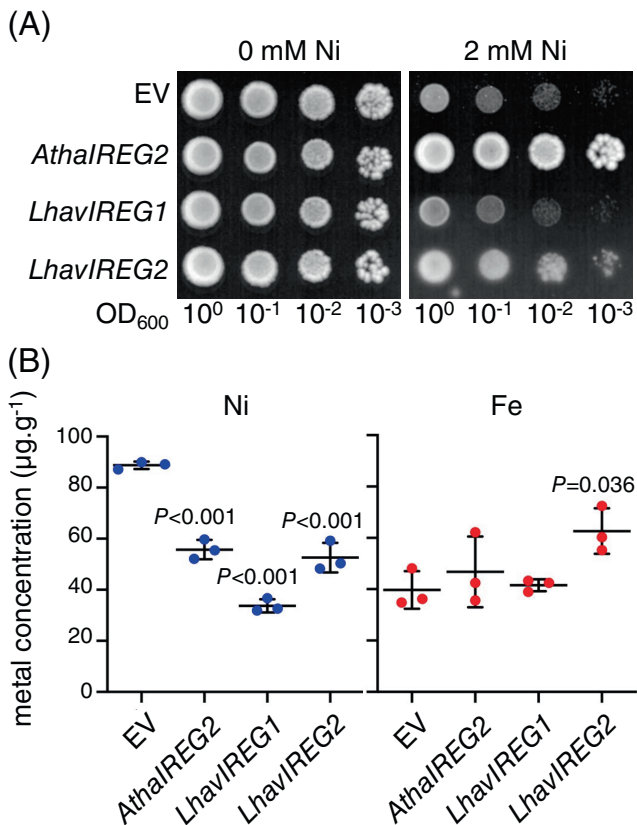


FIGURE 3 Nickel tolerance and accumulation in yeast cells expressing *LhaviREG1* and *LhaviREG2*. (A) Yeast cells expressing *LhaviREG1* and *LhaviREG2* were plated at different dilutions on media containing 0 and 2 mM NiCl₂. Yeast transformed with pDR195 vector (EV) and expressing *A. thaliana* *AthalREG2* were used as negative and positive control, respectively. (B) Nickel (blue) and iron (red) accumulation was measured by MP-AES in the same yeast lines. For each construct, the results are mean value \pm SD ($n = 3$ independent transformants). Adjusted P -values were calculated compared to the EV condition using a one-way ANOVA with Dunnett's post hoc multiple comparisons test at 95% confidence interval.

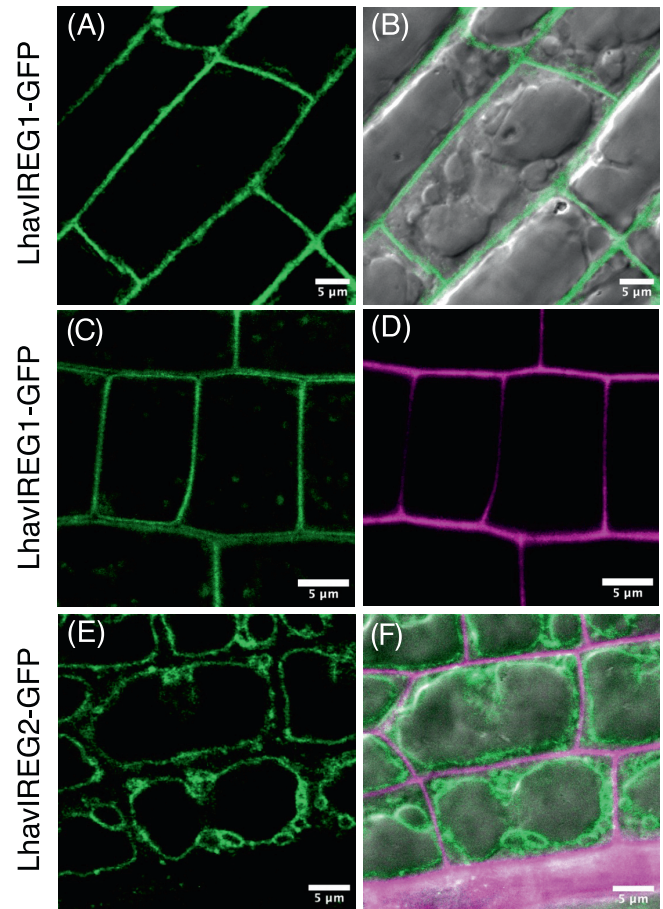
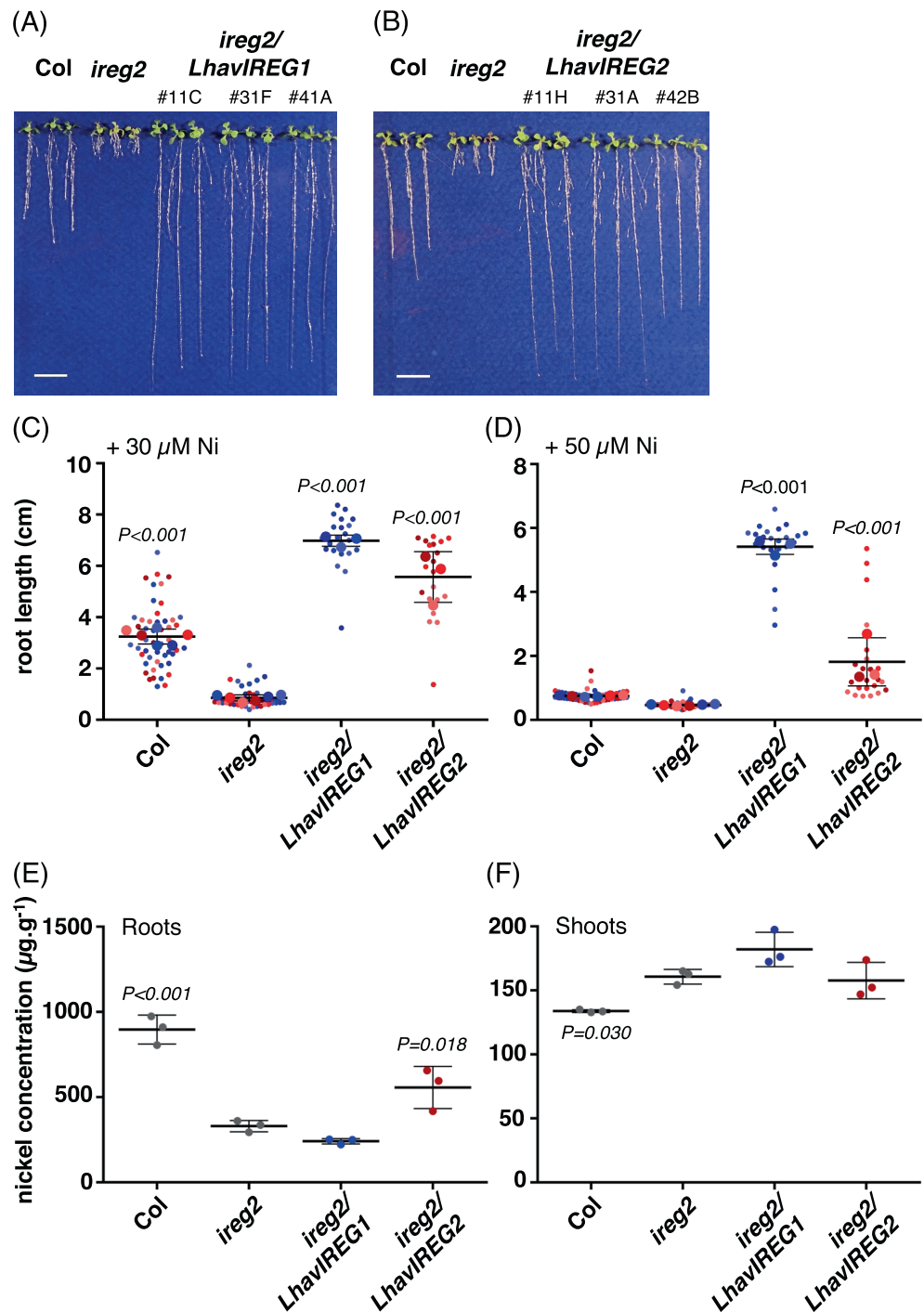


FIGURE 4 Localization of *LhaviREG1* and *LhaviREG2* in plant cells. Root cells of the *A. thaliana* *ireg2* mutant stably expressing *LhaviREG1*-GFP (2 independent transformants A, B and C, D) and *LhaviREG2*-GFP (E, F) were imaged by confocal microscopy. GFP-associated fluorescence is shown in green (A, C, E). Corresponding composite images with DIC images are also shown (B, F). Cell walls labelled with propidium iodine are shown in magenta (D, F). Scale bars are 5 µm.

FIGURE 5 Effect of LhaviREG1 and LhaviREG2 expression on nickel tolerance and accumulation. Pictures of individual *A. thaliana* *ireg2* transgenic lines expressing LhaviREG1-GFP (A) and LhaviREG2-GFP (B) grown on a culture medium containing 30 μM NiCl_2 for 10 days together with wild type (Col) and the *ireg2* mutant. Three representative plantlets were selected per line. Scale bars correspond to 1 cm. (C) Quantification of root growth of plantlets grown in the presence of 30 μM NiCl_2 and (D) 50 μM NiCl_2 . Each small dot represents an individual measurement. Large dots represent the mean value for each individual line or experiment. Means ($n = 3$ independent transgenic lines, $n = 6$ independent experiments for Col and *ireg2*) \pm SEM are shown. Adjusted P -values were calculated compared to *ireg2* using a one-way ANOVA with Dunnett's post hoc multiple comparisons test at 95% confidence interval. Nickel concentrations were measured in roots (E) and leaves (F) of the same genotypes. Data are mean value \pm SD ($n = 3$ independent transgenic lines). Adjusted P -values were calculated compared to *ireg2* using a one-way ANOVA with Dunnett's post hoc multiple comparisons test at 95% confidence interval.



This result suggests that LhaviREG2 is mainly localized on the vacuolar membrane. These results indicate that LhaviREG1 and LhaviREG2 localize to different membranes and therefore likely have different cellular functions.

3.6 | Expression of LhaviREG1 and LhaviREG2 in *A. thaliana* differentially affects nickel sensitivity and accumulation

We used the same *ireg2* transgenic lines expressing LhaviREG1-GFP and LhaviREG2-GFP to study the effect of the ubiquitous expression

of these transporters on nickel tolerance and accumulation (Figure 5). As observed in previous works (Schaaf et al. 2006; Merlot et al. 2014), the root growth of *A. thaliana* *ireg2* mutant is more sensitive to nickel than the wild type (Figure 5A-C). Expression of both LhaviREG1-GFP and LhaviREG2-GFP in *ireg2* significantly increases root growth in the presence of 30 μM nickel compared to *ireg2* or the wild-type (Figure 5A-D). In addition, transgenic lines expressing LhaviREG1-GFP and LhaviREG2-GFP do not exhibit the chlorotic phenotype observed in *ireg2* leaves in the presence of nickel. Transgenic lines expressing LhaviREG1-GFP show a strong tolerance up to 50 μM nickel, a concentration that strongly affects the root growth of LhaviREG2-GFP (Figure 5D).

To further characterize these transgenic lines, we measured nickel accumulation in both roots and shoots 5 days after transferring plants from a nickel-free medium to a medium containing 50 μM nickel (Figure 5E, F). The *ireg2* mutant, which is impaired in the vacuolar sequestration of nickel in roots, translocates more nickel into shoots than the wild type (Schaaf et al. 2006; Merlot et al. 2014). The expression of *LhaviREG2* in *ireg2* transgenic lines slightly increases nickel accumulation in roots but does not restore wild-type nickel accumulation, suggesting a partial complementation of the *ireg2* mutant for this phenotype. In contrast, expression of *LhaviREG1* does not restore nickel accumulation in roots compared to *ireg2*. In these experiments, *ireg2* contains more nickel in shoots than the wild type, but we did not observe a statistically significant effect of *LhaviREG1-GFP* and *LhaviREG2-GFP* expression on nickel accumulation compared to *ireg2* (Figure 5F). However, under these assay conditions, transgenic lines expressing *LhaviREG1-GFP* and *LhaviREG2-GFP* accumulate more iron and manganese in shoots than the *ireg2* mutant, likely reflecting their increased tolerance to nickel in shoots compared to *ireg2* (Figure S2). These results indicate that the ubiquitous expression of both *LhaviREG1* and *LhaviREG2* leads to a large increase in nickel tolerance, albeit through different cellular mechanisms (see discussion).

4 | DISCUSSION

In this work, we provided new insights into the function of the metal transporters of the IREG/FPN family, *LhaviREG1* and *LhaviREG2*, from the nickel hyperaccumulator species *Leucocroton havanensis* endemic from Cuba (Jestrow et al. 2012; González and Matrella 2013).

We generated a novel transcriptome assembly containing genes expressed in roots and shoots in this species (Table 1). Using this assembly as a reference, we examined the expression of genes in response to nickel in *L. havanensis* (Figure S1). Our results indicate that nickel treatment elicits a more complex response in shoots (442 DE genes) than in roots (27 DE genes). Enrichment analysis revealed that genes annotated as seed storage proteins are induced by nickel in roots (Table S2). The biological significance of this response remains unclear. No other functional category, including genes involved in the regulation of metal homeostasis, is enriched in response to nickel in roots or shoots.

Metal transporters of the IREG/FPN family have been implicated in the regulation of nickel homeostasis and tolerance in *A. thaliana* (Schaaf et al. 2006; Morrissey et al. 2009). More recently, the high expression of group 2 IREG/FPN was associated with the nickel hyperaccumulation trait in several plant families (Merlot et al. 2014; Meier et al. 2018; García de la Torre et al. 2021). In particular, *LhaviREG1* and *LhaviREG2* are more expressed in leaves of the nickel hyperaccumulator *L. havanensis* than *LmiclREG1*, the only detected group 2 IREG/FPN gene expressed in leaves of the closely related non-accumulator species *L. microphyllus* (García de la Torre et al. 2021). The analysis of the expression of *LhaviREG1* and *LhaviREG2* indicates that both genes are expressed at a similar level in leaves of *L. havanensis*, while *LhaviREG1* is more highly expressed than

LhaviREG2 in roots (Figure 2). qPCR experiments, however, revealed that nickel treatment moderately reduces *LhaviREG1* and *LhaviREG2* expression in shoots (Figure 2B). These results are consistent with a model suggesting that nickel hyperaccumulation at the species level is largely associated with a high and constitutive expression of genes involved in metal homeostasis and transport (Verbruggen et al. 2009; Krämer 2010), but we cannot exclude that nickel accumulation may exert a retro-control on the expression of genes involved in nickel transport in hyperaccumulator species.

We further investigated the function of *LhaviREG1* and *LhaviREG2* in nickel transport. Strong expression of *LhaviREG1* and *LhaviREG2* leads to a decrease in nickel accumulation in yeast as previously observed for *AthaliREG2* (Merlot et al. 2014). These results are consistent with the activity of *LhaviREG1* and *LhaviREG2* as metal exporters (Figure 3). However, the results obtained in yeast are difficult to interpret in a straightforward manner. One might expect that expression of a vacuolar form of IREG/FPN, such as *AthaliREG2*, would lead to increased nickel accumulation in yeast, which is not observed in our experiments (Figure 3B). Furthermore, expression of *LhaviREG1*, which reduces the net accumulation of nickel in yeast, does not increase nickel tolerance. These results suggest that plant IREG/FPN transporters are mistargeted in this heterologous expression system and that IREG/FPN expression, in addition to mediating a net efflux of nickel, may alter nickel distribution in different compartments of yeast and thus differentially affect nickel tolerance.

The expression of *LhaviREG1* and *LhaviREG2* tagged with GFP in transgenic *A. thaliana* plants indicates that *LhaviREG1* localizes at the plasma membrane, while *LhaviREG2* localizes on the vacuolar membrane (Figure 4). However, we cannot formally exclude that this localization does not accurately reflect the localization of these transporters in *Leucocroton havanensis*. The distinct localization of IREG/FPN transporters at the plasma membrane and at the vacuole was previously observed for *Arabidopsis thaliana* *AthaliREG1* and *AthaliREG2*, respectively (Schaaf et al. 2006; Morrissey et al. 2009). These observations suggest that in these two distant plant families, the duplication of an ancestral group 2 IREG/FPN gene resulted in transporters that convergently evolved into a plasma membrane and a vacuolar form. The molecular determinants of the cellular localization of IREG/FPN transporters are not yet known. Recently, the presence of a dileucine motif [D/E]X₃₋₅L[L/I] was shown to be involved in the vacuolar localization of *A. thaliana* NRAMP3 and NRAMP4 transporters (Bonifacino and Traub 2003; Komarova et al. 2012; Müdsam et al. 2018). At least three canonical dileucine motifs are found in the large cytoplasmic loop and C-terminal extension of *LhaviREG2* but not *LhaviREG1* (Figure S3). Further studies will be required to support the role of these motifs in the vacuolar localization of *LhaviREG2*.

As anticipated, the ectopic and constitutive expression of the vacuolar *LhaviREG2* increases nickel tolerance in the *A. thaliana* *ireg2* mutant (Figure 5B), as previously observed for *AthaliREG2* or *Psychotria gabriellae* PgIREG1 (Schaaf et al. 2006; Merlot et al. 2014). However, nickel dosage in roots and shoots (Figure 5E, F) further indicated that this phenotype is not simply the result of the complementation of the *AthaliREG2* function in roots but likely involves an increased

capacity of nickel storage and detoxification in the vacuoles of leaf cells. More surprisingly, the ectopic expression of the plasma membrane *LhavlREG1* increases nickel tolerance to a greater extent (Figure 5D). However, elemental analysis indicates that *LhavlREG1* expression does not restore nickel accumulation in roots compared to *ireg2* (Figure 5E). One hypothesis is that the ectopic expression of the plasma membrane *LhavlREG1* favors the translocation of nickel into the shoots. This function of *LhavlREG1* in metal translocation has previously been proposed for *A. thaliana* IREG1 (Morrissey et al. 2009). However, this hypothesis is difficult to validate with our experimental setup by measuring nickel accumulation in roots and shoots, because the *ireg2* mutant used as the genetic background for the transgenic lines already accumulates a low level of nickel in roots and translocates more nickel to shoots than the wild type (Figure 5E,F). Alternatively, the expression of *LhavlREG1* could mediate the export of nickel in the external medium. In leaves, the expression of *LhavlREG1* does not significantly alter the higher nickel accumulation observed in *ireg2* compared to wild type (Figure 6F), but reduces the toxicity associated with this accumulation (Figure 5A). Since *LhavlREG1* localizes to the plasma membrane, we propose that *LhavlREG1* exports nickel from leaf cells where it can bind to the cell wall. Interestingly, while the vacuolar sequestration of nickel is recognized as an essential function for nickel tolerance and hyperaccumulation (Schaaf et al. 2006; Merlot et al. 2014; García de la Torre et al. 2021), nickel is also associated with the cell wall in the leaves of several hyperaccumulators (Krämer et al. 2000; Bidwell et al. 2004; van der Ent et al. 2019). Additional experiments, including elemental imaging, would be required to support this hypothesis.

Taken together, our data show that the *Leucocroton havanensis* IREG/ferroportin transporters *LhavlREG1* and *LhavlREG2* are nickel exporters with distinct functions at the plasma membrane and vacuole of root and leaf cells. This represents a novel example of the neofunctionalization of metal transporters following the duplication of an ancestral gene (Logeman et al. 2017; Pottier et al. 2022). This duplication and neofunctionalization of a group 2 IREG/FPN transporter observed in the genus *Leucocroton* (Euphorbiaceae) appears to be convergent with that observed in Brassicaceae with *AthlREG1* and *AthlREG2*. Recently, the duplication of a transporter of the NRAMP family in the genus *Populus* (Salicaceae) and its neofunctionalization in two different membrane compartments was shown to be important for the regulation of manganese homeostasis (Pottier et al. 2022). These observations support the idea that the duplication and neofunctionalization of metal transporters is a common genetic phenomenon involved in the remarkable ability of plants to adapt to contrasting edaphic conditions. In the context of nickel hyperaccumulation, the function of both the vacuolar and plasma membrane forms of the group 2 IREG/FPN transporters may play complementary roles in the efficient translocation of nickel from the root to the shoots and in the accumulation and detoxification of nickel in the shoots.

AUTHOR CONTRIBUTIONS

DAG and SM: conceptualization; DAG, VSGT and SM: methodology; DAG, VSGT and SM: formal analysis; DAG, VSGT, RRF, LB and SM:

investigation; DAG: resources; VSGT and SM: data curation; DAG and SM: writing-review & editing; DAG, VSGT and SM: visualization; DAG, VSGT and SM: supervision; SM: funding acquisition.

ACKNOWLEDGEMENTS

We thank Ludivine Soubigou-Taconnat for the coordination of the *Leucocroton havanensis* RNA sequencing at the POPS platform (Orsay, France), Celeste Belloeil and Julien Spielmann for help with data presentation and Sébastien Thomine for comments on the manuscript.

FUNDING INFORMATION

This work was supported by the ANR funding EvoMetoNicks (ANR-13-ADAP-0004) and the MITI-CNRS Defi Enviromics GENE-4-CHEM to S.M. D.A.G and R.R.F were recipient of SCAC mobility fellowships from the French Embassy in Cuba.

DATA AVAILABILITY STATEMENT

The data discussed in this publication have been deposited in NCBI's Gene Expression Omnibus (Edgar et al. 2002) and are accessible through GEO Series accession number GSE237255 (<https://www.ncbi.nlm.nih.gov/geo/query/acc.cgi?acc=GSE237255>). Previous *Leucocroton* data (*Lhav_v1*) are available through GEO GSE116049. *LhavlREG1* and *LhavlREG2* cDNA sequences were deposited to GenBank under OR234317 and OR234318 accession numbers respectively.

ORCID

Dubiel Alfonso González  <https://orcid.org/0000-0003-4712-2016>

Vanesa Sánchez García de la Torre  <https://orcid.org/0000-0002-2972-6927>

Rolando Reyes Fernández  <https://orcid.org/0000-0003-2322-2901>

Sylvain Merlot  <https://orcid.org/0000-0002-9352-1184>

REFERENCES

- Becher M, Talke IN, Krall L, Krämer U (2004) Cross-species microarray transcript profiling reveals high constitutive expression of metal homeostasis genes in shoots of the zinc hyperaccumulator *Arabidopsis halleri*. *Plant J* 37: 251–268.
- Bidwell SD, Crawford SA, Woodrow IE, Sommer-Knudsen J, Marshall AT (2004) Sub-cellular localization of Ni in the hyperaccumulator, *Hybanthus floribundus* (Lindley) F. Muell. *Plant, Cell Environ* 27: 705–716.
- Bonifacino JS, Traub LM (2003) Signals for Sorting of Transmembrane Proteins to Endosomes and Lysosomes. *Annu Rev Biochem* 72: 395–447.
- Conte S, Stevenson D, Furner I, Lloyd A (2009) Multiple antibiotic resistance in *Arabidopsis* is conferred by mutations in a chloroplast-localized transport protein. *Plant Physiol* 151: 559–573.
- Corzo Remigio A, Chaney RL, Baker AJM, Edraki M, Erskine PD, Echevarria G, van der Ent A (2020) Phytoextraction of high value elements and contaminants from mining and mineral wastes: opportunities and limitations. *Plant Soil* 449: 11–37.
- Craciun AR, Meyer C-L, Chen J, Roosens N, De Groot R, Hilson P, Verbruggen N (2012) Variation in HMA4 gene copy number and expression among *Noccaea caerulea* populations presenting different levels of Cd tolerance and accumulation. *J Exp Bot* 63: 4179–4189.
- DalCorso G, Fasani E, Manara A, Visioli G, Furini A (2019) Heavy Metal Pollutions: State of the Art and Innovation in Phytoremediation. *Int J Mol Sci* 20: 3412.

- Dudka S, Adriano DC (1997) Environmental Impacts of Metal Ore Mining and Processing: A Review. *J Environ Qual* 26: 590–602.
- Edgar R, Domrachev M, Lash AE (2002) Gene Expression Omnibus: NCBI gene expression and hybridization array data repository. *Nucleic Acids Res* 30: 207–210.
- Edgar RC (2004) MUSCLE: multiple sequence alignment with high accuracy and high throughput. *Nucleic Acids Res* 32: 1792–1797.
- van der Ent A, Baker AJM, Reeves RD, Chaney RL, Anderson CWN, Meech JA, Erskine PD, Simonnot M-O, Vaughan J, Morel JL, Echevarria G, Fogliani B, Rongliang Q, Mulligan DR (2015) Agromining: Farming for Metals in the Future? *Environ Sci Technol* 49: 4773–4780.
- van der Ent A, Baker AJM, Reeves RD, Pollard AJ, Schat H (2013) Hyperaccumulators of metal and metalloids trace elements: Facts and fiction. *Plant Soil* 362: 319–334.
- van der Ent A, Spiers KM, Brueckner D, Echevarria G, Aarts MGM, Montargès-Pelletier E (2019) Spatially-resolved localization and chemical speciation of nickel and zinc in *Noccaea tymphaea* and *Bornmuelleria emarginata*. *Metalomics* 11: 2052–2065.
- Escudero V, Abreu I, Tejada-Jiménez M, Rosa-Núñez E, Quintana J, Prieto RI, Larue C, Wen J, Villanova J, Mysore KS, Argüello JM, Castillo-Michel H, Imperial J, González-Guerrero M (2020) Medicago truncatula Ferroportin2 mediates iron import into nodule symbiosomes. *New Phytol* 228: 194–209.
- García de la Torre VS, Majorel-Louergue C, Rigai GJ, Alfonso-González D, Soubigou-Taconnat L, Pillon Y, Barreau L, Thomine S, Fogliani B, Burtet-Sarramegna V, Merlot S (2021) Wide cross-species RNA-Seq comparison reveals convergent molecular mechanisms involved in nickel hyperaccumulation across dicotyledons. *New Phytol* 229: 994–1006.
- González DA, Matrella S (2013) Nickel hyperaccumulation ‘in vitro’ by *Leucocroton havanensis* (Euphorbiaceae) / Hiperacumulación ‘in vitro’ de Ni en *Leucocroton havanensis* (Euphorbiaceae). *Rev del Jardín Botánico Nac* 34/35: 83–88.
- Halimaa P, Lin Y-F, Ahonen VH, Blande D, Clemens S, Gyenesei A, Häikiö E, Kärenlampi SO, Laiho A, Aarts MGM, Pursiheimo J-P, Schat H, Schmidt H, Tuomainen MH, Tervahauta AI (2014) Gene expression differences between *Noccaea caerulescens* ecotypes help to identify candidate genes for metal phytoremediation. *Environ Sci Technol* 48: 3344–53.
- Hammond JP, Bowen HC, White PJ, Mills V, Pyke KA, Baker AJM, Whiting SN, May ST, Broadley MR (2006) A comparison of the *Thlaspi caerulescens* and *Thlaspi arvense* shoot transcriptomes. *New Phytol* 170: 239–260.
- Hanikenne M, Talke IN, Haydon MJ, Lanz C, Nolte A, Motte P, Kroymann J, Weigel D, Krämer U (2008) Evolution of metal hyperaccumulation required cis-regulatory changes and triplication of HMA4. *Nature* 453: 391–395.
- Jestrow B, Gutiérrez Amaro J, Francisco-Ortega J (2012) Islands within islands: a molecular phylogenetic study of the *Leucocroton* alliance (Euphorbiaceae) across the Caribbean Islands and within the serpentine archipelago of Cuba. *J Biogeogr* 39: 452–464.
- Kan M, Fujiwara T, Kamiya T (2022) Golgi-Localized OsFPN1 is Involved in Co and Ni Transport and Their Detoxification in Rice. *Rice* 15: 36.
- Kim LJ, Tsuyuki KM, Hu F, Park EY, Zhang J, Iraheta JG, Chia J, Huang R, Tucker AE, Clyne M, Castellano C, Kim A, Chung DD, DaVeiga CT, Parsons EM, Vatamaniuk OK, Jeong J (2021) Ferroportin 3 is a dual-targeted mitochondrial/chloroplast iron exporter necessary for iron homeostasis in *Arabidopsis*. *Plant J* 107: 215–236.
- Komarova NY, Meier S, Meier A, Grottemeyer MS, Rentsch D (2012) Determinants for *Arabidopsis* Peptide Transporter Targeting to the Tonoplast or Plasma Membrane. *Traffic* 13: 1090–1105.
- Krämer U (2010) Metal Hyperaccumulation in Plants. *Annu Rev Plant Biol* 61: 517–534.
- Krämer U, Pickering IJ, Prince RC, Raskin I, Salt DE (2000) Subcellular Localization and Speciation of Nickel in Hyperaccumulator and Non-Accumulator *Thlaspi* Species. *Plant Physiol* 122: 1343–1354.
- Letunic I, Bork P (2021) Interactive Tree Of Life (iTOL) v5: an online tool for phylogenetic tree display and annotation. *Nucleic Acids Res* 49: W293–W296.
- Li Z, Ma Z, van der Kuijp TJ, Yuan Z, Huang L (2014) A review of soil heavy metal pollution from mines in China: Pollution and health risk assessment. *Sci Total Environ* 468–469: 843–853.
- Logeman BL, Wood LK, Lee J, Thiele DJ (2017) Gene duplication and neofunctionalization in the evolutionary and functional divergence of the metazoan copper transporters Ctr1 and Ctr2. *J Biol Chem* 292: 11531–11546.
- Manara A, Fasani E, Furini A, DalCorso G (2020) Evolution of the metal hyperaccumulation and hypertolerance traits. *Plant Cell Environ* 43: 2969–2986.
- Meier SK, Adams N, Wolf M, Balkwill K, Muasya AM, Gehring CA, Bishop JM, Ingle RA (2018) Comparative RNA-seq analysis of nickel hyperaccumulating and non-accumulating populations of *Senecio coronatus* (Asteraceae). *Plant J* 95: 1023–1038.
- Merlot S, Hannibal L, Martins S, Martinelli L, Amir H, Lebrun M, Thomine S (2014) The metal transporter PglREG1 from the hyperaccumulator *Psychotria gabriellae* is a candidate gene for nickel tolerance and accumulation. *J Exp Bot* 65: 1551–1564.
- Morrissey J, Baxter IR, Lee J, Li L, Lahner B, Grotz N, Kaplan J, Salt DE, Guerinot M Lou (2009) The Ferroportin Metal Efflux Proteins Function in Iron and Cobalt Homeostasis in *Arabidopsis*. *Plant Cell* 21: 3326–3338.
- Müdsam C, Wollschläger P, Sauer N, Schneider S (2018) Sorting of *Arabidopsis* NRAMP3 and NRAMP4 depends on adaptor protein complex AP4 and a dileucine-based motif. *Traffic* 19: 503–521.
- ÓLochlainn S, Bowen HC, Fray RG, Hammond JP, King GJ, White PJ, Graham NS, Broadley MR (2011) Tandem Quadruplication of HMA4 in the Zinc (Zn) and Cadmium (Cd) Hyperaccumulator *Noccaea caerulescens*. *PLoS One* 6: e17814.
- Oomen RJFJ, Wu J, Lelièvre F, Blanchet S, Richaud P, Barbier-Brygoo H, Aarts MGM, Thomine S (2009) Functional characterization of NRAMP3 and NRAMP4 from the metal hyperaccumulator *Thlaspi caerulescens*. *New Phytol* 181: 637–650.
- Pan Y, Ren Z, Gao S, Shen J, Wang L, Xu Z, Yu Y, Bachina P, Zhang H, Fan X, Laganowsky A, Yan N, Zhou M (2020) Structural basis of ion transport and inhibition in ferroportin. *Nat Commun* 11: 5686.
- Pfaffl MW (2001) A new mathematical model for relative quantification in real-time RT-PCR. *Nucleic Acid Res* 29: 16–21.
- Pottier M, Le Thi VA, Primard-Brisset C, Marion J, Wolf Bianchi M, Victor C, Déjardin A, Pilate G, Thomine S (2022) Duplication of NRAMP3 Gene in Poplars Generated Two Homologous Transporters with Distinct Functions. *Mol Biol Evol* 39: 3737–3752.
- Reeves RD, Baker AJM, Jaffré T, Erskine PD, Echevarria G, Ent A (2018) A global database for plants that hyperaccumulate metal and metalloids trace elements. *New Phytol* 218: 407–411.
- Schaaf G, Honsbein A, Meda AR, Kirchner S, Wipf D, von Wirén N (2006) AtIREG2 Encodes a Tonoplast Transport Protein Involved in Iron-dependent Nickel Detoxification in *Arabidopsis thaliana* Roots. *J Biol Chem* 281: 25532–25540.
- Schwacke R, Ponce-Soto GY, Krause K, Bolger AM, Arsova B, Hallab A, Gruden K, Stitt M, Bolger ME, Usadel B (2019) MapMan4: A Refined Protein Classification and Annotation Framework Applicable to Multi-Omics Data Analysis. *Mol Plant* 12: 879–892.
- Seppy M, Manni M, Zdobnov EM (2019) BUSCO: Assessing Genome Assembly and Annotation Completeness BT - Gene Prediction: Methods and Protocols. In: Kollmar M (ed). *Springer* New York, New York, NY, pp. 227–245.

- Smith-Unna R, Boursnell C, Patro R, Hibberd J, Kelly S (2016) TransRate: reference free quality assessment of de novo transcriptome assemblies. *Genome Res* 26: 1134–1144.
- Sonter LJ, Dade MC, Watson JEM, Valenta RK (2020) Renewable energy production will exacerbate mining threats to biodiversity. *Nat Commun* 11: 6–11.
- Suman J, Uhlík O, Viktorova J, Macek T (2018) Phytoextraction of Heavy Metals: A Promising Tool for Clean-Up of Polluted Environment? *Front Plant Sci* 9: 1–15.
- Verbruggen N, Hermans C, Schat H (2009) Molecular mechanisms of metal hyperaccumulation in plants. *New Phytol* 181: 759–776.
- Vidal O, Le Boulzec H, Andrieu B, Verzier F (2022) Modelling the demand and access of mineral resources in a changing world. *Sustain* 14: 1–16.
- Weber M, Harada E, Vess C, Roepenack-Lahaye E V, Clemens S (2004) Comparative microarray analysis of *Arabidopsis thaliana* and *Arabidopsis halleri* roots identifies nicotianamine synthase, a ZIP transporter

and other genes as potential metal hyperaccumulation factors. *Plant J* 37: 269–281.

SUPPORTING INFORMATION

Additional supporting information can be found online in the Supporting Information section at the end of this article.

How to cite this article: González, D.A., de la Torre, V.S.G., Fernández, R.R., Barreau, L. & Merlot, S. (2024) Divergent roles of IREG/Ferroportin transporters from the nickel hyperaccumulator *Leucocroton havanensis*. *Physiologia Plantarum*, 176(2), e14261. Available from: <https://doi.org/10.1111/ppl.14261>